Intermolecular relaxation has little effect on intra-peptide exchange-transferred NOE intensities

Adam P.R. Zabell[a] & Carol Beth Post[a,b,*]

[a]*Department of Medicinal Chemistry and Molecular Pharmacology, Purdue University, West Lafayette, IN 47907-1333 U.S.A.;* [b]*Department of Biological Sciences, Purdue University, West Lafayette, I 47907-1392, U.S.A.*

Abstract

Exchange-transferred nuclear Overhauser enhancement (etNOE) provides a useful method for determining the 3-dimensional structure of a ligand bound to a high-molecular-weight complex. Some concern about the accuracy of such structures has arisen because indirect relaxation can occur between the ligand and macromolecule. Such indirect relaxation, or spin diffusion, would lead to errors in interproton distances used as restraints in structure determination. We address this concern by assessing the extent of intermolecular spin diffusion in nineteen peptide-protein complexes of known structure. Transferred NOE intensities were simulated with the program CORONA (Calculated OR Observed NOESY Analysis) using the rate-matrix approach to include contributions from indirect relaxation between protein-ligand and intraligand proton pairs. Intermolecular spin diffusion contributions were determined by comparing intensities calculated with protonated protein to those calculated with fully deuterated protein. The differences were found to be insignificant overall, and to diminish at short mixing times and high mole ratios of peptide to protein. Spin diffusion between the peptide ligand and the protein contributes less to the etNOE intensities and alters fewer cross peaks than the well-studied intramolecular spin diffusion effects. Errors in intraligand interproton distances due to intermolecular relaxation effects were small on average and can be accounted for with the restraint functions commonly used in NMR structure determination methods. In addition, a rate-matrix approach to calculate distances from etNOESY intensities using a volume matrix comprising only intraligand intensities was found to give accurate values. Based on these results, we conclude that structures determined from etNOESY data are no less accurate due to spin diffusion than structures determined from conventional NOE intensities.

Abbreviations: etNOE – exchange-transferred nuclear Overhauser enhancement; CORONA – program for Calculated or Observed NOESY Analysis.

Introduction

Exchange-transferred nuclear Overhauser enhancement (etNOE) (Balaram et al., 1972a, Clore and Gronenborn, 1982, 1983) provides a useful method for determining the 3-dimensional structure of a ligand bound to a very high-molecular-weight complex in so-lution (Campbell and Sykes, 1993, Lian et al., 1994). For exchange involving a ligand, L, and protein, P,

$$P + L \underset{k_{\text{off}}}{\overset{k_{\text{on}}}{\rightleftharpoons}} PL, \tag{1}$$

where k_{off} is the dissociation rate constant and k_{on} is the association rate constant. The application of this methodology has grown substantially in recent years, particularly with regard to determining peptide

*To whom correspondence should be addressed. E-mail: cbp@purdue.edu

304

structures bound to proteins as a model for protein-protein interactions. The etNOE method is important for gaining structural information about systems that are too large for direct observation by NMR, or otherwise not amenable to study by high-resolution NMR or X-ray crystallography. In the bound state, the ligand adopts a long correlation time and cross relaxation between ligand protons becomes significant. Although the NOE signal develops in the bound state, it is measured through ligand exchange by observing the relatively narrow ligand resonances of the free state. Fast exchange of the ligand between associated and dissociated states is required for the simplest interpretation of the etNOE experiment. A reasonable estimate for satisfying the condition of fast exchange is an equilibrium dissociation constant (k_{off}/k_{on}) of 10 μM or higher. NOE cross peaks from protein protons are not observed since both the free protein and the PL complex are often too high in molecular weight. Further, given a free ligand that has a rotational correlation time near the inverse field strength of the NMR spectrometer, the NOE of free ligand is insignificant and the NOE intensity is a function of interligand proton distances in the bound state. This distance information, combined with restrained simulated annealing molecular dynamics, is sufficient for determining bound peptide structures in peptide-protein complexes (Eisenmesser et al., 2000).

As with conventional NOE data, indirect cross relaxation between multiple spin pairs can alter the et-NOE cross peak of the ligand proton pair defining the direct interaction. How an indirect relaxation pathway influences the etNOE cross peak intensity depends on whether the additional spin is from the ligand or the macromolecule (London et al., 1992; Zheng and Post, 1993, 1995; Liu et al., 1995; Moseley et al., 1995). For some spatial arrangements of spins, the indirect contribution is greater when the additional spin is from the macromolecule rather than the ligand (Zheng and Post, 1993). In the case of conventional NOE measurements, this spin diffusion can be taken into account in the calculation of interproton distances by using a rate matrix analysis of the NOE intensity, although it is more frequent that the errors in distance estimates arising from spin diffusion are accounted for through an appropriate restraint potential function. In the case of etNOE measurements, the use of a rate matrix analysis is uncertain since the cross peak intensities from the protein are not generally observable. This point and the relatively large indirect effect that can arise from intermolecular relaxation have lead to

some concern about the accuracy of interproton distances determined from etNOESY intensities and the reliability of the resulting ligand structure (Arepalli et al., 1995; Jackson et al., 1995). There are instances where intermolecular spin diffusion was reported to have altered some experimental cross peak volumes (Zheng and Post, 1993; Barsukov et al., 1996; Vincent et al., 1997; Sokolowski et al., 1998). In one case a ligand structure was wrongly determined because of a distance that was estimated incorrectly as a result of intermolecular spin diffusion (Glaudemans et al., 1990; Arepalli et al., 1995). One approach to avoid intermolecular spin diffusion is to replace protein hydrogen atoms with deuterium atoms (Shibata et al., 1995; Barsukov et al., 1996), although it should be noted that incomplete deuteration of the protein complicates the use of a full matrix analysis of the system (Zolnai et al., 1998).

To determine how prevalent intermolecular spin diffusion might be, we performed a detailed study of the effects of spin diffusion using nineteen peptide-protein complexes with structures determined by X-ray crystallography. Relative to co-factors and certain other small-molecule ligands, peptide ligands can have a larger number of NOE interactions and often bind on the protein surface. For each peptide-protein complex, peak intensities were simulated using coordinates from the PDB (Berman et al., 2000) by a rate matrix approach with the program CORONA (Calculated OR Observed NOESY Analysis) to include all intermolecular and intramolecular proton interactions in an exchange system. The effects on ligand interproton distance estimates due to both intermolecular and intramolecular spin diffusion were assessed. From these complexes we determined that although intermolecular spin diffusion is present in every system, it is smaller in magnitude and less prevalent than intramolecular spin diffusion and with a few basic precautions should not adversely affect the determination of peptide ligand structures. In addition, the simulated intraligand etNOESY intensities were placed back into a rate matrix analysis to calculate distances by an approach that could be implemented experimentally. The results showed that such an analysis comprising only intraligand cross peak volumes yields reasonably accurate values for distances.

Theory and methods

Exchange-transferred NOESY

The time-dependent etNOE intensity is described by the Bloch equations (Bloch, 1957) with the addition of chemical exchange terms (Clore and Gronenborn, 1982, 1983). The matrix that includes all pairwise interactions in a multiple-spin system undergoing exchange accounts for spin diffusion among those spins (Landy and Rao, 1989; London et al., 1992; Zheng and Post, 1993; Ni and Zhu, 1994; Jackson et al., 1995). The evolution of the etNOESY intensity as a function of the mixing time t_m is

$$\frac{\mathrm{d}}{\mathrm{d}t_m}\mathbf{V}(t_m) = -\mathbf{\Gamma}\mathbf{V}(t_m). \tag{2}$$

The elements of the matrix $\mathbf{V}(t_m)$ are the peak volumes of the etNOESY spectrum while terms in the rate matrix $\mathbf{\Gamma}$ include the exchange rates k_{on} and k_{off}, as well as the off-diagonal cross-relaxation rate σ_{ij} between proton i and j,

$$\sigma_{ij} = \frac{\gamma_H^4 \hbar^2}{10 r_{ij}^6}(6J(2\omega) - J(0)) \tag{3}$$

and the diagonal self-relaxation term ρ_i

$$\rho_i = \sum_{j \neq i}^{N} \frac{\gamma_H^4 \hbar^2}{10 r_{ij}^6}(6J(2\omega) + 3J(\omega) + J(0)). \tag{4}$$

The distance between the two protons is r_{ij}, the gyromagnetic ratio for hydrogen is γ_H, and the spectral density function is $J(\omega)$ for frequency ω.

When exchange is fast relative to the magnetic relaxation rates, the effective relaxation rate is the sum of the rate in the free and bound form of the molecule weighted by the mole fraction of the two forms. That is, for the case of i and j ligand spins, the effective cross-relaxation rate, $\sigma_{ij}^{\mathrm{avg}}$, is

$$\sigma_{ij}^{\mathrm{avg}} = \left(\frac{[PL]\sigma_{ij}^b}{[L]_T}\right) + \left(\frac{([L]_T - [PL])\sigma_{ij}^f}{[L]_T}\right). \tag{5}$$

The superscripts f and b denote the free and bound state of the molecules, respectively. The subscript T denotes the total concentration of the molecule. In this fast-exchange limit, the relaxation–plus-exchange rate matrix in Equation 2 can be symmetrized (Landy and Rao, 1989): For n-spin ligand and m-spin protein molecules, Equation 2 simplifies to a set of

$(n + m)$ differential equations that include ligand-protein cross-relaxation contributions in a symmetrical rate matrix (Zheng and Post, 1993):

$$\frac{\mathrm{d}}{\mathrm{d}t_m}\begin{bmatrix} (\mu_p^b)^{-1/2}(\mathbf{V}_l^b + \mathbf{V}_l^f) \\ (\mu_l^b)^{-1/2}(\mathbf{V}_p^b + \mathbf{V}_p^f) \end{bmatrix} =$$

$$-\begin{bmatrix} \mu_l^b \Gamma_l^b + \mu_l^f \Gamma_l^f & (\mu_l^b \mu_p^b)^{1/2}\Gamma_{lp}^b \\ (\mu_l^b \mu_p^b)^{1/2}\Gamma_{pl}^b & \mu_p^b \Gamma_p^b + \mu_p^f \Gamma_p^f \end{bmatrix} \tag{6}$$

$$\times \begin{bmatrix} (\mu_p^b)^{-1/2}(\mathbf{V}_l^b + \mathbf{V}_l^f) \\ (\mu_l^b)^{-1/2}(\mathbf{V}_p^b + \mathbf{V}_p^f) \end{bmatrix}.$$

The subscripts l and p refer to ligand and protein hydrogens, respectively. Γ_l^b and Γ_l^f are symmetrical $n \times n$ relaxation matrices for the ligand. Similarly, Γ_l^b and Γ_l^f are symmetrical $m \times m$ relaxation matrices for the protein. The diagonal elements ρ_i in Γ_l^b and Γ_p^b include both intramolecular and intermolecular dipolar interactions in their summation (Equation 4). Γ_{lp}^b and Γ_{pl}^b are $n \times m$ and $m \times n$ rate matrices, respectively, that contain cross-relaxation rates between protein and ligand protons in the complex. The four μ terms are relative concentration ratios for each of the compounds in the system at chemical equilibrium

$$\mu_l^b = \frac{[PL]}{[PL] + [L]} \tag{7}$$

$$\mu_l^f = \frac{[L]}{[PL] + [L]} \tag{8}$$

$$\mu_p^b = \frac{[PL]}{[PL] + [P]} \tag{9}$$

$$\mu_p^f = \frac{[P]}{[PL] + [P]}. \tag{10}$$

Hereafter, $\mathbf{V}(t_m)$ refers to the matrix on the left side of Equation 6, while Γ refers to the first matrix on the right side of Equation (6). The calculation of etNOE peak intensities given cross-relaxation rates based on a three-dimensional structure, as well as the inverse calculation of rates from intensities, was performed using the program CORONA (Zheng and Post, 1993; Eisenmesser et al., 2000). CORONA is capable of similar analysis of conventional NOE systems as well.

Reference X-ray structures

A keyword search of the PDB (Berman et al., 2000; http://www.rcsb.org/pdb) as of January 2000 identified

Table 1. Nineteen PDB complexes for which etNOESY intensities were simulated

PDB code	Description	Complex M_r (kDa)	Whole peptide M_r (kDa)	Residues in simulation	Primary source
1A5G	α-thrombin with hirugen	37.3	1.4	2–12	St. Charles et al., 1999
1ACB	α-chymotrypsin with eglin c	37.6	8.4	37–51	Frigerio et al., 1992
1ATP	cAMP-dependent protein kinase with pki(5-24)	44.8	2.4	1–20	Zheng et al., 1993
1B2S	Barnase with barstar	71.7	10.8	25–50	Buckle et al., 1994
1BBR	α-thrombin with fibrinopeptide(7-16)	101.2	1.3	1–10	Martin et al., 1992
1BMQ	Interleukin-1b convertase with peptidomimetic inhibitor	31.0	0.5	1–5	Okamoto et al., 1999
1BRS	Barnase with a barstar double mutant	71.3	10.6	25–47	Buckle et al., 1994
1CHO	α-chymotrypsin with OMTKY3	35.9	6.7	10–23, 29–37	Fujinaga et al., 1987
1EKB	Enteropeptidase with trypsinogen activation peptide analog	30.5	0.7	2–6	Lu et al., 1999
1PEK	Proteinase K with substrate analog	34.0	0.7	1–5	Betzel et al., 1993
1QUR	Thrombin with bivalent inhibitor	36.1	2.2	1–22	Steinmetzer et al., 1999
1SHD	C-Src SH2 domain with inhibitor	13.6	0.7	1–5	Gilmer et al., 1994
1SMF	Trypsin with Bowman-Birk peptide	29.3	2.6	9–17	Li et al., 1994
1SMR	Rennin with rat angiotensinogen-based inhibitor	41.1	1.1	1–9	Dealwis et al., 1994
2PTC	β-trypsin with BPTI	33.6	6.9	10–21, 32–40	Marquart et al., 1983
2SIC	Subtilisin BPN' with streptomyces subtilisin inhibitor	45.7	12.8	64–77, 95–102	Takeuchi et al., 1991
4CPA	Carboxypeptidase A with potato inhibitor	41.4	4.5	21–38	Rees and Lipscomb, 1982
4ER4	Endothiapepsin with a rennin inhibitor	40.6	1.2	1–9	Foundling et al., 1987
4SGB	Serine proteinase B with potato inhibitor	28.4	6.1	1–10, 27–44	Greenblatt et al., 1989

peptide-protein complexes solved by X-ray crystallography to 2.5 Å or better resolution. Complexes with peptides less than 5 residues, redundant entries, and entries for which the protein was mutated at residues away from the molecular interface were discarded. A barnase:barstar complex (PDB entry 1BRS) with two mutations in the binding site (Buckle et al., 1994) was included along with the wild-type complex. A total of nineteen complexes were investigated. The PDB code, a brief description of each complex, and the molecular weight of both ligand and complex is given in Table 1. In those systems with ligand molecular weights larger than 2.6 kDa, the ligand size was reduced for the simulation of etNOE intensities in order to resemble the size of peptide ligands used in etNOE studies. Larger molecular weight ligands undergo efficient cross-relaxation in the free state which would lead to a free-state NOE intensity and complicate the interpretation of the etNOE data. For the eight complexes 1ACB, 1B2S, 1BRS, 1CHO, 2PTC, 2SIC, 4CPA and 4SGB, only ligand residues which formed the longest continuous peptide within 8 Å of the protein were included in the calculations. If one Cys residue of a disulphide bridge fell within the 8 Å cutoff, both strands containing the disulphide-

Cys residues were included. The ligand residues used in the simulation with CORONA are also listed in Table 1. Some complexes contained cofactors. Cofactor atoms were treated as protein atoms. Hydrogens were built onto the crystallographic coordinates using QUANTA (Accelrys Inc.). The structures were subjected to 100 steps of energy minimization using the all hydrogen CHARMM22 parameters (Brooks et al., 1983, MacKerell et al., 1998) and fixing all non-hydrogen atoms.

Simulation of exchange-transferred NOESY

This study focuses on the effects of spin diffusion in the fast exchange limit and independent of molecular weight. While the dependence on exchange rate and correlation time was not investigated, these factors could be examined in future studies. Exchange-transferred NOE intensities were simulated for a total protein concentration of 0.5 mM and a total ligand concentration of 5.0 mM under fast exchange conditions; k_{off} equaled 1000 s^{-1} and k_{on} was set to the diffusion limit of 10^8 M^{-1} s^{-1}. The correlation time for the free ligand and for the complex was 0.625 nsec and 35 nsec, respectively, for all complexes. A constant value typical for molecules examined by etNOE

methods was used independent of the actual molecular weight of the complex in order to eliminate correlation time as a variable. The mixing time was 100 ms and the spectrometer frequency was 750 MHz. The effects of mixing time and peptide-protein ratio were examined using the 1ATP (Zheng et al., 1993) and 4ER4 (Foundling et al., 1987) complexes. For these systems, etNOE spectra were calculated at 100, 200 and 500 ms mixing times and peptide-protein ratios equal to 5:1, 10:1, and 20:1. The protein concentration was 0.5 mM for each ratio.

Peak volumes were calculated from the solution to Equation 6 with the program CORONA using relaxation rates estimated from interproton distances obtained from the X-ray complex. Hydrogens in fast exchange with water from Ser, Thr, and Tyr sidechains, and protein hydrogens greater than 8.0 Å away from any ligand atom were excluded from the calculations. The resulting systems included between 315 and 908 protein spins and between 27 and 198 ligand spins for the nineteen complexes. The systems were treated as rigid bodies except that the rotation of methyl groups was modeled by the average $\langle r_{ij}^{-3}\rangle^2$ over the three methyl sites as previously described (Post, 1992). Methylene protons, as well as $H\delta$ and $H\epsilon$ protons on tyrosine and phenylalanine residues, were assumed to have degenerate chemical shifts. This assumption was made because the chemical shifts of methylene protons are either actually degenerate or their stereospecific assignments are not generally made. Thus, these intensities were averaged over the individual simulated values.

Two sets of etNOE intensities were calculated for each complex. The first included both peptide and protein hydrogens in the matrix to simulate typical experimental conditions, while the second was obtained using peptide hydrogens but no protein hydrogens in order to simulate experimental conditions as if the protein were deuterated. A comparison was made between these spectra to determine the extent of intermolecular spin diffusion in each complex. Intensities were converted to interproton distances using a reference intensity and distance on the peptide with the ratio

$$\frac{I_{ij}}{I_{\text{reference}}} = \frac{r_{\text{reference}}^6}{r_{ij}^6}.$$ (11)

The preferred reference (Post, 1992) is an $H\delta$-$H\epsilon$ intensity of tyrosine or phenylalanine with the distance of 2.54 Å. If there was no aromatic ring on the ligand,

a geminal intensity at a fixed distance of 1.75 Å was used.

Intramolecular spin diffusion was also monitored as previously described (Post et al., 1990). The indirect relaxation via ligand protons is assessed by comparing distances calculated from Equation 11 using intensities simulated for a deuterated protein to the actual distances in the X-ray structure.

Calculation of the rate-matrix and distances from peak volumes

The solution to the differential Equation 6 equates the volume matrix $\mathbf{V}(t_m)$ to a function of Γ, which is generated for a given structure. By appropriate rearrangement of this solution, one obtains the expression for Γ as a function of the etNOESY intensities, $\mathbf{V}(t_m)$. The r_{ij} value corresponding to σ_{ij}^{avg} is obtained from Equations 5 and 3. This analytical approach for estimating distances was executed whereby only intraligand etNOE intensities were included in the volume matrix in order to investigate the reliability of rates and distances estimated from a volume matrix lacking intensities for protein protons. The intraligand peak volumes were from simulations based on the full 1ATP or 4ER4 complex with a 10:1 peptide-protein ratio, 100 ms mixing time, and the remaining parameter values as specified above. The rate-matrix was calculated from $\mathbf{V}(t_m)$ comprising diagonal peak volumes for each ligand proton and either all intrapeptide cross peak volumes or only those intrapeptide volumes greater than a threshold value corresponding to 5% of the reference cross peak. Motional averaging of methyl groups was included.

Error determination

Root mean square deviations, ε, were evaluated for intraligand distances or cross-relaxation rates

$$\varepsilon = \sqrt{\frac{\sum_{i}^{N}(s1_i - s2_i)^2}{N}},$$ (12)

where $s1$ and $s2$ are the compared values and N is the number of pairs. Comparison was made between two calculated values, or between a calculated value and the actual value known from the structure of the complex. The sum was over pairs separated less than 5 Å in the X-ray structure, or approximately 25 etNOE interactions per peptide residue on average.

Results and discussion

Computer simulation of NMR relaxation properties in macromolecules is useful for identifying contributions from intermolecular relaxation pathways and spin diffusion to etNOE intensities (London et al., 1992; Zheng and Post, 1993; Jackson et al., 1995). The utility of this procedure was demonstrated with NADH:LDH (Zheng and Post, 1993) for which an intermolecular spin diffusion pathway was predicted from simulations and subsequently observed experimentally (Vincent et al., 1997).

Intermolecular and intramolecular spin diffusion in etNOESY spectra

Exchange-transferred NOE intensities, $\mathbf{V}(t_m)$, were simulated according to Equation 6 for the nineteen complexes listed in Table 1 in order to identify the extent of intermolecular and intramolecular spin diffusion. Intermolecular spin diffusion via the protein is eliminated when protons on the protein are substituted for deuterium atoms. Thus, a straightforward analysis of intermolecular spin diffusion is achieved by comparison of intensities simulated using a protonated protein with those using a deuterated protein while keeping all other parameters constant. Rather than a discussion of difference intensities in arbitrary values, comparison is made in terms of distance values obtained from the inverse sixth power of the intensities and a reference intensity from a fixed-distance interaction within the complex (Equation 11). For comparison, indirect effects from multispin relaxation within the ligand were also assessed. The intensities simulated with the deuterated protein complex were used to assess the errors due to indirect intraligand interactions; the difference between the distance calculated from a two-spin approximation (Equation 11) and the actual distance in the X-ray structure (Post et al., 1990) is the error due to intramolecular spin diffusion.

The influence of ligand-protein spin diffusion is illustrated in Figure 1b by a comparison of distance values estimated from intensities obtained with either the protonated-protein complex or the deuterated-protein complex. The deviations from the diagonal are due to indirect relaxation pathways involving protein protons. Plots are shown for the complexes 1ATP (Zheng et al., 1993) (left column) and 4ER4 (Foundling et al., 1987) (right column). The other complexes exhibited deviations that in general ranged between these

two examples. For all complexes, at least 90% of the distances agree within 0.5 Å, and no significant differences are found for distances less than ∼3.5 Å. The effect of indirect relaxation from protein protons is to underestimate certain intraligand distances. That the intensities in the protonated-protein spectrum are stronger than those in the deuterated-protein spectrum is consistent with the presence of a protein proton closer to the direct intraligand protons than the intraligand pair itself. A detailed discussion of the factors involved has been described (Zheng and Post, 1993).

Intramolecular effects lead to the deviations shown in Figure 1c for 1ATP and 4ER4. Immediately apparent is the larger dispersion in Figure 1c for intramolecular spin diffusion compared to that seen for intermolecular spin diffusion in Figure 1b. A larger number of interactions fall off the diagonal and the deviations occur over the full range of interactions. The tendency that results from intramolecular spin diffusion is to overestimate distances less than the reference distance, and to underestimate longer distances (Post et al., 1990).

The number of deviations greater than 0.1 and 0.5 Å, and an r.m.s. error (ε) are provided in Table 2 for each complex. The values are tabulated by error due to intermolecular spin diffusion or intramolecular spin diffusion, and the total error from the combination of both inter- and intramolecular spin diffusion. On average, 7% of the distances had errors greater than 0.5 Å as a result of peptide-protein relaxation. Only two complexes, 1EKB (Lu et al., 1999) and 1PEK (Betzel et al., 1993), had more than 15% of the distances with deviations of this magnitude. Notably, in more than two-thirds of the complexes, the errors from spin diffusion through the protein affected only one or two peptide residues, and often only one to three atoms. Thus, the inaccuracies are localized and not likely to influence the entire peptide structure. For example, in 2PTC (Marquart et al., 1983) 28 of 388 distances are mis-assigned by 0.5 Å or more due to intermolecular contributions to the cross peak intensities; 21 of these intensities are from Lys 15, and thirteen intensities are from either Hα or the Hγ∗ geminal proton pair. This residue has an extended conformation and binds into a pocket of the protein where extensive intermolecular interactions take place. By comparison, intramolecular spin diffusion leads to a substantially larger number of errors (Table 2); on average 17% of the proton distances deviated by more than 0.5 Å. Unlike spin diffusion between peptide and protein, indirect relaxation generated within the peptide affects etNOE intensities
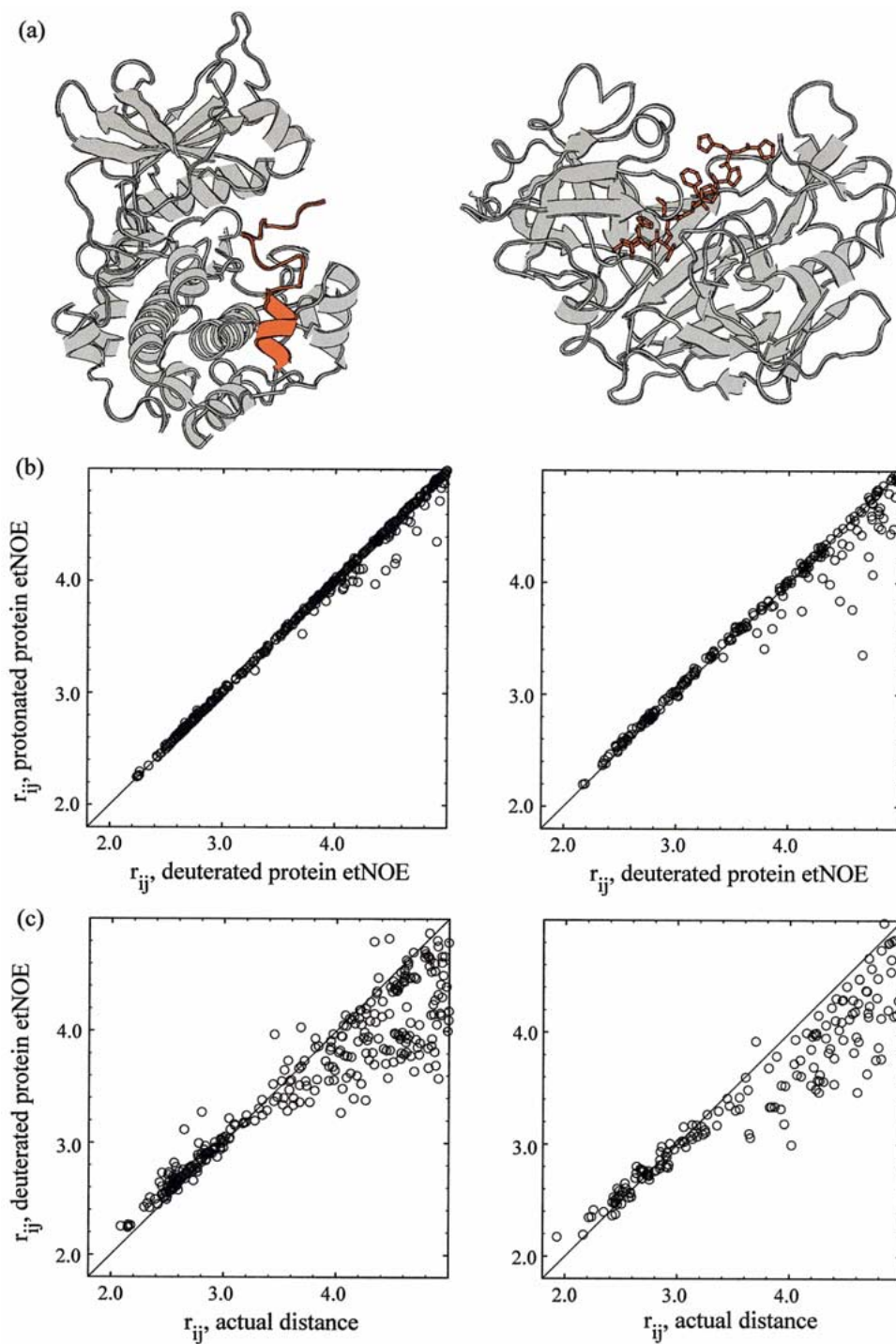
Figure 1. Values of peptide interproton distances to illustrate effects from intermolecular and intramolecular spin diffusion in the complex of cAMP-dependent protein kinase with pki(5-24) (PDB 1ATP) (Zheng et al., 1993) (left-hand panels) and endothiapepsin with rennin inhibitor (PDB 4ER4) (Foundling et al., 1987) (right-hand panels). (a) Ribbon diagrams of the protein (grey) and the peptide (red). Side-chains are not shown for 1ATP to better show the α-helical portion of the peptide. (b) Plot of ligand interproton distances calculated from a ratio of the etNOE intensities simulated for either protonated or deuterated protein. Deviations from the diagonal are due to spin diffusion via intermolecular relaxation pathways. (c) Ligand interproton distances calculated from a ratio of the etNOE intensities simulated for deuterated protein against the actual distance in the reference structure. Deviations from the diagonal are due to spin diffusion within the peptide ligand. The number of peaks affected by intramolecular spin diffusion is substantially larger than those affected by intermolecular spin diffusion.

Table 2. Number of distances with errors above a threshold value and the r.m.s. error, ε[a]

PDB code	No. NOEs	Intermolecular[b]		Intramolecular[c]		ε, Å		
		$\Delta > 0.1$ Å	$\Delta > 0.5$ Å	$\Delta > 0.1$ Å	$\Delta > 0.5$ Å	Intermol.[b]	Intramol.[c]	Overall[d]
1A5G	214	25	5	89	24	0.06	0.37	0.36
1ACB	389	60	32	148	44	0.17	0.41	0.36
1ATP	406	28	5	171	62	0.05	0.41	0.40
1B2S	397	38	14	158	53	0.13	0.44	0.41
1BBR	275	51	13	130	47	0.08	0.50	0.49
1BMQ	198	59	28	116	48	0.13	0.59	0.56
1BRS	402	40	11	169	38	0.09	0.34	0.32
1CHO	399	49	20	179	67	0.08	0.44	0.42
1EKB	69	31	15	40	25	0.19	0.95	0.86
1PEK	80	32	18	31	6	0.20	0.39	0.30
1QUR	1260	137	51	663	291	0.06	0.53	0.52
1SHD	85	9	1	40	13	0.14	0.38	0.35
1SMF	366	96	41	178	118	0.13	0.89	0.86
1SMR	450	114	53	251	99	0.14	0.46	0.45
2PTC	388	57	28	170	51	0.14	0.39	0.36
2SIC	415	54	22	165	61	0.09	0.40	0.39
4CPA	521	46	19	231	68	0.06	0.39	0.38
4ER4	233	48	13	101	35	0.15	0.42	0.38
4SGB	369	13	8	152	46	0.05	0.36	0.35

[a]See Equation 12.
[b]Differences between the distance calculated from spectra simulated with protonated versus deuterated protein.
[c]Differences between the actual distance in the X-ray structure and distance calculated from the spectrum simulated with deuterated protein.
[d]Differences between the actual distance and distance calculated from the spectrum simulated with protonated protein.

from multiple residues and atoms. The rms error from intramolecular spin diffusion is between two and eight times larger than the error from intermolecular spin diffusion. Interestingly, the overall rms error is slightly less than that due only to intramolecular spin diffusion, indicating that intermolecular spin diffusion counterbalances intramolecular spin diffusion. It was shown using a three-spin model (Zheng and Post, 1993) that indirect relaxation through the protein enhances the etNOE intensity but does not diminish it. Thus the compensation in error must arise from an enhancement due to intermolecular effects and a loss of etNOE intensity due to intramolecular effects.

The distribution of the errors from either inter- (black) or intramolecular (red) spin diffusion in the 19 complexes is shown in Figure 2. The profiles differ considerably in their nature. Most intermolecular spin diffusion errors are insignificant and less than 0.02 Å (see inset), while errors from intramolecular relaxation are more uniformly distributed and account for most of the errors between 0.1 Å and 1.2 Å. A small number of errors have values greater than 1.6 Å,
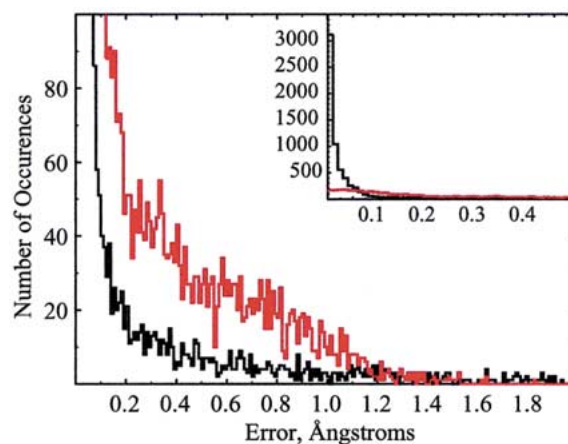

Figure 2. Distribution of the errors in 19 peptide-protein complexes (see Table 1). Errors due to intermolecular (black line) and intramolecular (red line) spin diffusion are shown. The inset to the figure shows that the vast majority of intermolecular effects occur at less than 0.05 Å.

and most of these arise from intermolecular pathways. Because the occurrence of large inaccuracies in distances is rare ($\sim 1\%$ of the etNOEs), potential errors

may become evident during the structure determination process from inconsistencies between the poorly defined restraints and the majority of other etNOE distances.

Ratio and mixing time dependence

Most etNOESY studies acquire spectra with a mixing time of 100–200 ms and peptide-protein ratios of approximately 10:1 (Ni, 1994). Some reports (Clore and Gronenborn, 1982; Lian et al., 1994) suggest a ratio larger than 10:1 should be used provided nonspecific interactions can be avoided, although there is disagreement on the benefit of such a large excess (Campbell and Sykes, 1993; Jackson et al., 1995). The dependence of intermolecular relaxation on mixing time and peptide-protein mole ratio was investigated to determine whether indirect contributions could be reduced under certain conditions. The 1ATP complex and the 4ER4 complex were selected for this analysis since the peptide in 1ATP lies on the surface of the protein, while the peptide in 4ER4 is buried under two loops in the protein structure. The extensive contact surface in 4ER4 leads to the larger deviations from the diagonal in Figure 1c and the larger intermolecular ε value (Table 2).

The errors were determined at peptide-protein mole ratios 5:1, 10:1 and 20:1, and mixing times 100 ms, 200 ms, and 500 ms for 1ATP or 4ER4. These values are within the range reported in the literature but it should be noted that, at smaller mixing times and higher peptide to protein ratios, experimental signal-to-noise decreases, leading to significant error in the measured intensity. The r.m.s. value for the error from intermolecular and intramolecular spin diffusion, as well as the net overall contribution are provided as a function of peptide-protein ratio and mixing time for both 1ATP and 4ER4 in Table 3. The trend is toward smaller errors for higher peptide ratios and shorter mixing times. The r.m.s. error for intermolecular spin diffusion is roughly three times higher for the buried peptide in 4ER4 than for the surface-bound peptide in 1ATP at a given ratio and mixing time. At 100 ms and the 20:1 ratio, for instance, ε for 1ATP is 0.05 Å and 0.15 Å for 4ER4. While the effect of intermolecular relaxation differs between the two complexes, the overall and intramolecular values of ε for 1ATP and 4ER4 are roughly the same and independent of binding nature; the overall error ranges between 0.3 Å at 100 ms and 20:1 and 1.2 Å at 500 ms and 5:1 for both complexes. To illustrate the trends in more detail,

the distribution of the overall error scaled to the actual distance is shown in Figure 3 for 4ER4. The errors are less severe as the peptide-protein ratio increases. At longer mixing time (black to red to green trace in Figure 3a–c), the error distribution flattens and extends to larger values.

Rate-matrix analysis limited to intraligand interactions

The rate-matrix Equation 6 takes into account multiple, simultaneous dipolar interactions leading to spin diffusion, and may be solved for either Γ or $\mathbf{V}(t_m)$. The results discussed above refer to etNOESY intensities $\mathbf{V}(t_m)$ simulated by including all relaxation elements in Γ from a given peptide-protein structure. The experimentalist requires the inverse operation of determining Γ given the intensities $\mathbf{V}(t_m)$. The accuracy in the σ_{ij} values of Γ determined from NOE intensities decreases when the matrix $\mathbf{V}(t_m)$ is incomplete (Post et al., 1990). In the case of etNOESY data, a complete set of intensities cannot be measured since protein cross peaks are usually too broad to observe. Nevertheless, it is of interest to consider a rate-matrix analysis that includes only the data which can be measured in an etNOE experiment: The intraligand NOE intensities. The question we address is whether reliable distance estimates can be obtained from a rate-matrix analysis based on an incomplete volume matrix comprising only intraligand intensities. The finding that the contributions from intermolecular spin diffusion are insignificant for the majority of etNOE intensities (Figures 1b and 2) encourages the use of such an approach. A rate-matrix analysis of the observed intraligand etNOE interactions would account for intramolecular spin diffusion, the major indirect contribution to the NOE intensity, and should therefore lead to reasonable estimates of distances.

To test this approach, an incomplete volume matrix with only intraligand intensities was used to solve the differential Equation 6 for Γ, or more specifically, the ligand cross-relaxation rates under fast-exchange conditions. The intraligand intensities were simulated using the relaxation rates calculated from the full complex coordinate set for 1ATP or 4ER4, a 10:1 ratio of peptide-protein concentration, and a 100 ms mixing time. The ligand interproton distance, r_{ij}, was calculated from σ_{ij}^{avg} (Equation 5), a function of both a free and a bound cross-relaxation rate. For simplicity, it was assumed that the interproton distance in σ_{ij}^{free} and σ_{ij}^{bound} is equal. Although the distance in the free state

Table 3. R.m.s. error, ε, as a function of mixing time and peptide ratio

	1ATP, RMSD[a]			4ER4, RMSD[a]		
	Intermol.	Intramol.	Overall	Intermol.	Intramol.	Overall
100 ms, 5:1	0.05	0.58	0.58	0.15	0.56	0.56
100 ms, 10:1	0.05	0.41	0.40	0.15	0.42	0.38
100 ms, 20:1	0.05	0.30	0.28	0.15	0.32	0.25
200 ms, 5:1	0.07	0.78	0.80	0.19	0.75	0.81
200 ms, 10:1	0.05	0.57	0.56	0.16	0.57	0.55
200 ms, 20:1	0.06	0.42	0.40	0.17	0.43	0.38
500 ms, 5:1	0.13	1.12	1.19	0.32	1.05	1.23
500 ms, 10:1	0.07	0.82	0.84	0.20	0.81	0.86
500 ms, 20:1	0.05	0.61	0.60	0.17	0.62	0.60

[a]Terms defined in Table 2.

Table 4. R.m.s. error, ε, in calculated rates and distances from a rate matrix analysis of intraligand etNOESY volumes

	$\varepsilon, \sigma_{ij}^{avg}$		ε, r_{ij}	
	All volumes	$V_{threshold}$	All volumes	$V_{threshold}$
1ATP				
Deuterated protein	1.9×10^{-3}	6.6×10^{-2}	0.002	0.157
Protonated protein	2.0×10^{-2}	8.7×10^{-2}	0.135	0.241
4ER4				
Deuterated protein	4.0×10^{-5}	7.2×10^{-3}	0.001	0.104
Protonated protein	7.4×10^{-2}	1.0×10^{-1}	0.176	0.227

is likely to vary, this assumption is inconsequential since σ_{ij}^{free} is small relative to σ_{ij}^{bound} due to the respective correlation times. Accuracy was assessed from the rms deviations between cross-relaxation rates, and corresponding interproton distances, calculated from the ligand-only volume matrix versus the actual values obtained from the X-ray structure. Results are shown in Table 4 for 1ATP and 4ER4.

Errors in σ_{ij}^{avg} arise from two sources of incompleteness in the volume matrix: the loss of information on ligand-protein interactions and the experimental limitation of measuring intraligand interactions at long range. The calculation of Γ from intensities obtained with deuterated protein eliminates errors due to loss of ligand-protein information since there is no intermolecular relaxation. Including all simulated etNOESY intensities in the calculation with no cutoff on the intraligand cross peak intensities eliminates errors due to missing these long-range interactions. Thus, a solution for Γ was determined from both the full set of

intraligand peak intensities as well as a subset of those intensities above a threshold value corresponding to 5% of the reference intensity. As shown in Table 4, when the deuterated protein model is used with no cutoff on the etNOE intensity, the error for 1ATP and 4ER4 in σ_{ij}^{avg} of 1.9×10^{-3} and 4.0×10^{-5} and in r_{ij} of 0.002 Å and 0.001 Å, respectively, is neglibly small and due to numerical error. In the realistic case in which the intraligand volume matrix includes only intensities above a certain threshold value, the error increases even in the absence of indirect relaxation via protein protons: the uncertainty in the distances is 0.16 and 0.10 Å for 1ATP and 4ER4, respectively. When the etNOESY intensities are obtained with protonated protein, the error in the estimated distances relative to that from intensities obtained with deuterated protein is greater, but remains small overall. In the case of the surface-bound peptide in 1ATP, the error increases from 0.16 Å to 0.24 Å, while the error for the predominantly buried peptide in 4ER4 increases by a factor of
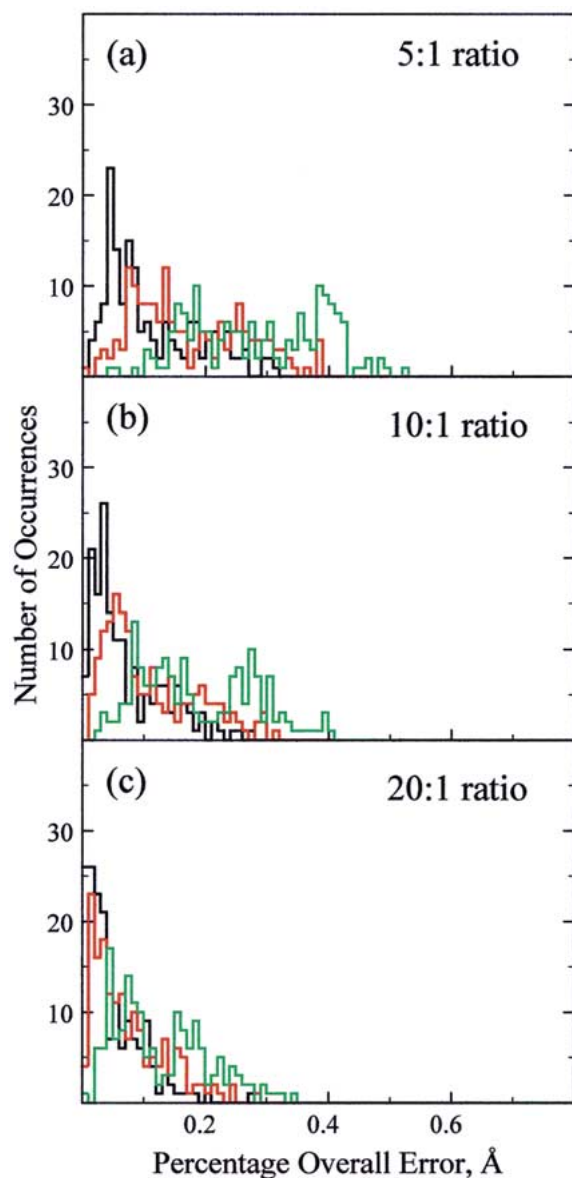
Figure 3. Distribution of the overall error in the calculated ligand interproton distance scaled to the actual value for different peptide:protein mole ratios and mixing time of an etNOESY experiment. Distances are calculated from the ratio of etNOESY intensities simulated for protonated protein. Values are shown for peptide:protein ratios of (a) 5:1, (b) 10:1 and (c) 20:1. The scaled error corresponds to 100 ms (black line), 200 ms (red line), and 500 ms (green line) mixing times. The scaled error tends to smaller values as either the ratio increases or the mixing time decreases.

two from 0.10 Å to 0.23 Å. Although the uncertainty produced from truncation of long-range intraligand interactions is similar in magnitude to that from the presence of protein protons, the total error is considerably smaller than the value of ~ 0.4 Å shown in Table 2 for distances estimated from intensities ratios, i.e., a two-spin approximation (Equation 11).

Conclusions

The etNOESY method is extremely useful for obtaining structural information on large biological complexes not amenable to conventional NOE studies or crystallization. We have examined the potential for indirect relaxation contributions to etNOESY intensities due to intermolecular relaxation pathways in order to determine the accuracy of ligand interproton distances estimated from etNOE intensities and thus the reliability implied for the bound peptide structures. Here, we used a simulation study of fast chemical exchange and nineteen peptide-protein complexes that exhibit a wide variety of binding arrangements, including peptides that are predominantly buried, as in the complexes 4ER4 and 1BBR, and those that extend along the surface, as in the complexes 1ATP and 1QUR. The results show that intermolecular relaxation affects the accuracy of distances (estimated from a ratio of etNOE intensities) significantly less than indirect relaxation within the exchanging peptide. Interestingly, the contributions to certain cross peaks from intermolecular and intramolecular spin diffusion are opposite in direction and thus compensate to give smaller overall error in the distance value.

A rate-matrix solution for ligand interproton distances determined from a volume matrix $\mathbf{V}(t_m)$ that contains only the intraligand cross peak intensities was found to be more accurate than distances based on the intensity ratios. However, the errors in this matrix approach were more evenly distributed between apparent intermolecular and intramolecular effects, as might be expected from a simultaneous solution of multiple equations.

Inaccuracies in distance restraints due to intramolecular spin diffusion have long been accounted for in structure determination by the use of a square-well restraint function with upper and lower bounds set by estimates in the error. Such restraint functions would compensate for intermolecular spin diffusion effects equally well since these effects were found to be fewer in number and no larger in magnitude than

314

intramolecular effects. Both strong/medium/weak categorization of distances based on observed intensities, and a rate-matrix calculation to estimate distances are accurate within the restraint bounds already employed in the established structure-determination programs X-PLOR/CNS and DYANA. Thus, the van der Waals radius as a lower limit and a generous upper limit for distance categories (Brünger, 1992), or slightly tighter bounds for rate-matrix based, individual restraints (Liu et al., 1995; Güntert et al., 1997) are appropriate. In this study, large inaccuracies due to intermolecular spin diffusion did occur; in less than 1% of the distances errors greater than 1.6 Å were found, but these errors were most often distances involving a single side chain. Together, these findings suggest that errors caused by intermolecular relaxation may become evident during the structure determination process due to conflicts between the erroneous restraint and the other etNOE restraints. Such conflicts would point out a need to re-evaluate those restraints.

A matter for concern regarding structures determined from either conventional NOE or exchange-transferred NOE intensities is the situation when too few NOE interactions exist. For any restraint-based method, regions of the system that are poorly defined experimentally must be viewed cautiously and with careful consideration of the undue influence from a single, possibly erroneous, NOE restraint. The structural correction published by Arepalli et al. (1995), for example, was necessitated because previous work had defined the relative orientation of the two sugar rings in a disaccharide with a single restraint. In the case of peptide-protein complexes, several etNOE interactions are most often observed for each peptide residue, but the consequence of sparse etNOE restraints should also be recognized (Eisenmesser et al., 2000).

When intermolecular spin diffusion is suspected, approaches are available to ensure that critical etNOE restraints are free from intermolecular spin diffusion effects: complete deuteration of the protein, or by quenching spin diffusion through the use of the QUIET-NOESY experiment (Vincent et al., 1997) are reliable approaches. It is noted that the QUIET-NOESY method requires *a priori* knowledge of the resonant frequencies of the direct and indirect spins.

Acknowledgements

References

Arepalli, S.R., Glaudemans, C.P.J., Daves, Jr., G.D., Kovac, P. and Bax, A. (1995) *J. Magn. Reson.*, **B106**, 195–198.

Balaram, P., Bothner-By, A.A. and Breslow, E. (1972a) *J. Am. Chem. Soc.*, **94**, 4017–4018.

Balaram, P., Bothner-By, A.A. and Dadok, J. (1972b) *J. Am. Chem. Soc.*, **94**, 4015–4017.

Barsukov, I.L., Lian, L.Y., Ellis, J., Sze, K.H., Shaw, W.V. and Roberts, G.C.K. (1996) *J. Mol. Biol.*, **262**, 543–558.

Berman, H.M., Westbrook, J., Feng, Z., Gilliland, G., Bhat, T.N., Weissig, H., Shindyalov, I.N. and Bourne, P.E. (2000) *Nucl. Acids Res.*, **28**, 235–242.

Betzel, C., Singh, T.P., Visanji, M., Peters, K., Fittkau, S., Saenger, W. and S., W.K. (1993) *J. Biol. Chem.*, **268**, 15854–15858.

Bloch, F. (1957) *Phys. Rev.*, **105**, 1206–1222.

Brooks, B.R., Bruccoleri, R.E., Olafson, B.D., States, D.J., Swaminathan, S. and Karplus, M. (1983) *J. Comput. Chem.*, **4**, 187–217.

Brünger, A.T. (1992) *X-PLOR 3.1: A System for X-Ray Crystallography and NMR,* Yale University Press, New Haven, CT.

Buckle, A.M., Schreiber, G. and Fersht, A.R. (1994) *Biochemistry*, **33**, 8878–8889.

Campbell, A.P. and Sykes, B.D. (1993) *Annu. Rev. Biophys. Biomol.*, **22**, 99–122.

Clore, G.M. and Gronenborn, A.M. (1982) *J. Magn. Reson.*, **1982**, 402–417.

Clore, G.M. and Gronenborn, A.M. (1983) *J. Magn. Reson.*, **53**, 423–442.

Dealwis, C.G., Frazao, C., Badasso, M., Cooper, J.B., Tickle, I.J., Driessen, H., Blundell, T.L., Murakami, K., Miyazaki, H., Sueirasdiaz, J., Jones, D.M. and Szelke, M. (1994) *J. Mol. Biol.*, **236**, 342–360.

Eisenmesser, E.Z., Zabell, A.P.R. and Post, C.B. (2000) *J. Biomol. NMR*, **17**, 17–32.

Foundling, S.I., Cooper, J., Watson, F.E., Cleasby, A., Pearl, L.H., Sibanda, B.L., Hemmings, A., Wood, S.P., Blundell, T.L., Valler, M.J., Norey, C.G., Kay, J., Boger, J., Dunn, B.M., Leckie, B.J., Jones, D.M., Atrash, B., Hallett, A. and Szelke, M. (1987) *Nature*, **327**, 349–352.

Frigerio, F., Coda, A., Pugliese, L., Lionetti, C., Menegatti, E., Amiconi, G., Schnebli, H.P., Ascenzi, P. and Bolognesi, M. (1992) *J. Mol. Biol.*, **225**, 107–123.

Fujinaga, M., Sielecki, A.R., Read, R.J., Ardelt, W., Laskowski, M. and James, M.N.G. (1987) *J. Mol. Biol.*, **195**, 397–418.

Gilmer, T., Rodriquez, M., Jordan, S., Crosby, R., Alligood, K., Green, M., Kimery, M., Wagner, C., Kinder, D., Charifson, P., Hassell, A.M., Willard, D., Luther, M., Rusnak, D., Sternbach, D.D., Mehrotra, M., Peel, M., Shampine, L., Davis, R., Robbins,

J., Patel, I.R., Kassel, D., Burkhart, W., Moyer, M., Bradshaw, T. and Berman, J. (1994) *J. Biol. Chem.*, **269**, 31711–31719.

Glaudemans, C.P.J., Lerner, L., Daves, Jr., G.D., Kovác, P., Venable, R. and Bax, A. (1990) *Biochemistry*, **29**, 10906–10911.

Greenblatt, H.M., Ryan, C.A. and James, M.N.G. (1989) *J. Mol. Biol.*, **205**, 201–228.

Güntert, P., Mumenthaler, C. and Wüthrich, K. (1997) *J. Mol. Biol.*, **273**, 283–298.

Jackson, P.L., Moseley, H.N.B. and Krishna, N.R. (1995) *J. Magn. Reson. B*, **107**, 289–292.

Landy, S.M. and Rao, B.D.N. (1989) *J. Magn. Reson.*, **81**, 371–377.

Li, Y.L., Huang, Q.C., Zhang, S.W., Liu, S.P., Chi, C.W. and Tang, Y.Q. (1994) *J. Biochem. Tokyo*, **116**, 18–25.

Lian, L.Y., Barsukov, I.L., Sutcliffe, M.J., Sze, K.H. and Roberts, G.C.K. (1994) *Meth. Enzymol.*, **239**, 657–700.

Liu, H., Spielmann, P., Ulyanov, N.B., Wemmer, D.E. and James, T.L. (1995) *J. Biomol. NMR*, **6**, 390–402.

London, R.E., Perlman, M.E. and Davis, D.G. (1992) *J. Magn. Reson.*, **97**, 79–98.

Lu, D.S., Futterer, K., Korolev, S., Zheng, X.L., Tan, K., Waksman, G. and Sadler, J.E. (1999) *J. Mol. Biol.*, **292**, 361–373.

MacKerell, A.D.J., Bashford, D., Bellott, M., Dunbrack, R.L., Evanseck, J.D., Field, M.J., Fischer, S., Gao, J., Guo, H., Ha, S., Joseph-McCarthy, D., Kuchnir, L., Kuczera, K., Lau, F.T.K., Mattos, C., Michnick, S., Ngo, T., Nguyen, D.T., Prodhom, B., Reiher, W.E., Roux, B., Schlenkrich, M., Smith, J.C., Stote, R., Straub, J. and Karplus, M. (1998) *J. Phys. Chem.*, **B102**, 3586–3616.

Marquart, M., Walter, J., Deisenhofer, J., Bode, W. and Huber, R. (1983) *Acta Crystallogr.*, **B39**, 480–490.

Martin, P.D., Robertson, W., Turk, D., Huber, R., Bode, W. and Edwards, B.F.P. (1992) *J. Biol. Chem.*, **267**, 7911–7920.

Moseley, H.N.B., Curto, E.V. and Krishna, N.R. (1995) *J. Magn. Reson.*, **B108**, 243–261.

Ni, F. (1994) *Prog. NMR Spectr.*, **26**, 517–606.

Ni, F. and Zhu, Y. (1994) *J. Magn. Reson.*, **B103**, 180–184.

Okamoto, Y., Anan, H., Nakai, E., Morihira, K., Yonetoku, Y., Kurihara, H., Sakashita, H., Terai, Y., Takeuchi, M., Shibanuma, T. and Isomura, Y. (1999) *Chem. Pharm. Bull.*, **47**, 11–21.

Post, C.B. (1992) *J. Mol. Biol.*, **224**, 1087–1101.

Post, C.B., Meadows, R.P. and Gorenstein, D.G. (1990) *J. Am. Chem. Soc.*, **112**, 6796–6803.

Rees, D.C. and Lipscomb, W.N. (1982) *J. Mol. Biol.*, **160**, 475–498.

Shibata, C.G., Gregory, J.D., Gerhardt, B.S. and Serpersu, E.H. (1995) *Arch. Biochem. Biophys.*, **319**, 204–210.

Sokolowski, T., Haselhorst, T., Scheffler, K., Weisemann, R., Kosma, P., Brade, H., Brade, L. and Peters, T. (1998) *J. Biomol. NMR*, **12**, 123–133.

St. Charles, R., Matthews, J.H., Zhang, E.L. and Tulinsky, A. (1999) *J. Med. Chem.*, **42**, 1376–1383.

Steinmetzer, T., Renatus, M., Kunzel, S., Eichinger, A., Bode, W., Wikstrom, P., Hauptmann, J. and Sturzebecher, J. (1999) *Eur. J. Biochem.*, **265**, 598–605.

Takeuchi, Y., Satow, Y., Nakamura, K.T. and Mitsui, Y. (1991) *J. Mol. Biol.*, **221**, 309–325.

Vincent, S.J.F., Zwahlen, C., Post, C.B., Burgner, J.W., II and Bodenhausen, G. (1997) *Proc. Natl. Acad. Sci. USA*, **94**, 4383–4388.

Zheng, J. and Post, C.B. (1993) *J. Magn. Reson.*, **B101**, 262–270.

Zheng, J. and Post, C.B. (1996) *J. Phys. Chem.*, **100**, 2675–2680.

Zheng, J.H., Trafny, E.A., Knighton, D.R., Xuong, N.H., Taylor, S.S., Teneyck, L.F. and Sowadski, J.M. (1993) *Acta Crystallogr.*, **D49**, 362–365.

Zolnai, Z., Juranic, N. and Macura, S. (1998) *J. Biomol. NMR*, **12**, 333–337.